Development of an adaptive aerofoil contour for use as a fan blade

JANNIS MÜLLER
M.Eng.

H. HAHN
Prof. Dr.-Ing.

C. FRIEBE
Dipl.-Ing.

Keywords: Adaptive aerofoil, axial fan, flow separation, force measurements

Abstract

This article about a master thesis represents a contribution to the development of axial fans with adaptive blade profiles. The adaptive blade profiles should be able to be changed in operation so that high efficiency is achieved not only at the design point, but also in the partial load range of the fan operation. Studies on the effectiveness of such blades are held to reduce the complexity of stationary aerofoils.

The search concludes that aerofoils which have a function of adjusting their angle of attack and the additional function of adapting their profile curvature would be particularly suitable for the use on rotating systems. In order to prove this assessment, force measurements are carried out on two reference profiles and finally are compared with an adaptive aerofoil profile developed for this purpose. For these measurements, a separate test rig was set up and validated, which allows equivalent investigations on dormant aerofoil profiles.

The three profiles were developed according to Carolus and designed for the production with a 3D printer using CAD software.

In the final part, investigations are carried out with a laser-optical measuring method in order to reveal potential for improvement in future research.

With an overall assessment of the effect of the adaptive aerofoil, as well as a recommendation for the use of the potentials, this work contributes to the further development of axial fans with adaptive blade profiles.

This article is the winner of REHVA Student Competition award, see news on page 90.

I. Introduction

A. Basics about fans

Fans are flow machines designed to transport gaseous fluids. They are often used in recooling systems or decentralised ventilation systems. Also, for special applications such as mine ventilation or in wind tunnels, axial fans are used because of their performance in the transport of large volume flows [4]. The task of mass transport fans should meet with a certain volume flow at a given pressure difference. This design point is regularly used to define the type of flow machines. When designing building services, it is common practice to design the fans to peak performance with an additional safety margin to ensure building operation at full capacity. However, it is realistic that the facilities will not work at the design point but mainly in a part load operation. Manufacturer of fans take this into account and therefore develop the blades of a fan in their shape so that they work not at the design point, but at a certain load point with maximum efficiency [6]. However, high efficiency would not be desirable in points, but over a load range between the part load and the design point.

In addition to business economic motivation, environmental policy also plays a role in the design of fans. For example, following the identification of a significant potential for improving the environmental impact of energy-related products, the European Commission also adopted a regulation on the environmentally sound design of fans. Since the regulation (EU) Nr. 327/2011 came into effect, the requirements on the environmentally sound design of fans are according to the directive 2009/125/EG lawfully defined [2]. With a measured system efficiency, axial fans with a power consumption of 125 W ≤ P_{el} ≤ 10 kW currently has to meet a target efficiency is given by equation (1) with

$$\eta_{target} = 2{,}74 \ln(P) - 6{,}33 + N \qquad (1)$$

where P is the electrical power consumption in kW and N is a prescribed degree of efficiency (static N = 40).

The efficiency tests take place on standardised test setups, whereby the data is recorded with optimal efficiency [2].

It is conceivable that such static test methods will be replaced by methods with dynamic load distribution in the future and thus the target efficiency must be met not at an optimal point, but in different ranges. If the efficiency requirements for fans continue to rise in the future, then the research on fan blades with adjustable curvature while running will be not only very useful, but also an important step in the development of a more efficient generation of flow machines.

This work contributes to the development of adjustable blade contours for use in axial fans. The focus of the work is the development of an adjustable blade and the proof of an improvement of partial load behaviour. For this, a test setup must be developed and verified. Corresponding examinations and test series should prove the effectiveness of the adjustable blade.

B. Working principle of fan blades

”Everybody moving in a fluid experiences a force. Of interest are those bodies which - in addition to a low drag force against the direction of movement - have a high lift force perpendicular to the direction of movement. Planar bodies with these properties, whose dimensions in one direction - the “thickness” of the body - are much smaller than in the two perpendicular directions - the “depth” and the “span” - are called “aerofoils”. A section perpendicular to the span direction may be called “aerofoil profile” or “profile” for short.” [10].

During the flow around a profile, different speed and pressure conditions occur along its surface. The air is accelerated when displaced, the dynamic pressure increases, and the static pressure decreases according to the energy conservation. The pressure field along the surface is therefore crucial for the resulting lift force.

Fan blades operate on the principle of an aerofoil and typically have an asymmetric curvature. The force resulting from the pressure gradients expresses as lift force on the blades which is necessary for the transportation of the fluid. The one-sided curvature generates a drop in static pressure in front of the fan. A good aerofoil contour is characterised by high lift force with low drag force.

The glide ratio

$$\varepsilon = \frac{W}{A} \ , \qquad (2)$$

is an indicator for the rating of different contours. The thickening of profiles as well as the increase of its curvature results in an unfavourable glide ratio [5].

C. Fan-characteristics

The flow properties of fans are described with fancharacteristics. These describe the possible operating points of a fan from free-air point ($\dot{V} = max$, $\Delta p = 0$) to stagnation point ($\dot{V} = 0$, $\Delta p = max$) at a specific speed. **Figure 1** shows a schematic fan-characteristic with loss fractions where the operating point is optimally located at the point of least loss. Often only the static pressures without losses are indicated in the fan characteristics.

For an optimal operation of fans, the sum of hydraulic losses Z_h must be minimised through a net-adapted blade configuration on the impeller. The impellers work Y_{Sch} then transfers to the fluid as much as possible.

$$Y = Y_{Sch} - Z_h = \frac{\Delta p_t}{\rho} \qquad (3)$$

It is:

Y = the spec. Nozzle-work (between suction and discharge nozzles)

Y_{Sch} = the mass-specific work by the fan blades

Z_h = the sum of the hydraulic losses

Δp_t = the increase of total pressure [9]

Unlike fan-characteristics, system characteristic curves describe the resistance to be overcome for transporting fluids generated by friction in the network. Each fluid system has a characteristic which, with

$$\Delta p = \frac{\rho}{2} v^2 \qquad (4)$$

is a quadratic function of velocity. The intersection of the fan characteristic with the line characteristic is the operating point.

A change in the system characteristic can, for example, by actuation of a throttle damper, but also caused by contamination. The connection between the volume flow and the necessary support work in the fluid system then changes and new operating points are created.

Figure 2 shows the fan-characteristic of an axial fan according to BANZHAF [3] at a constant speed and a constant blade angle in a system with a continuously closing throttle damper. With an opened throttle, the fan works at operation point (1) with low pressure loss and high volume flow. With increasing throttling, the operating point on the fan characteristic rises above (2) and (3) to point (4). At point (5) the fan works with maximum pressure increase on the stable part of its characteristic curve. With further throttling the flow separates from the fan blades and the pressure increase suddenly drops. In order to return the fan from the unstable characteristic curve at point (7) to the stable characteristic curve, the throttle must be opened until point (8) has been reached. Only from (9), the flow again can be close on the blades, whereby the fan changes back into its stable characteristic range.

Instable operating areas of the axial fan lead to socalled pumping which causes an increased oscillatory load. This manifest itself in acoustic problems, damage to the duct system or damage to the suspension, bearings and blades of the fan [3].

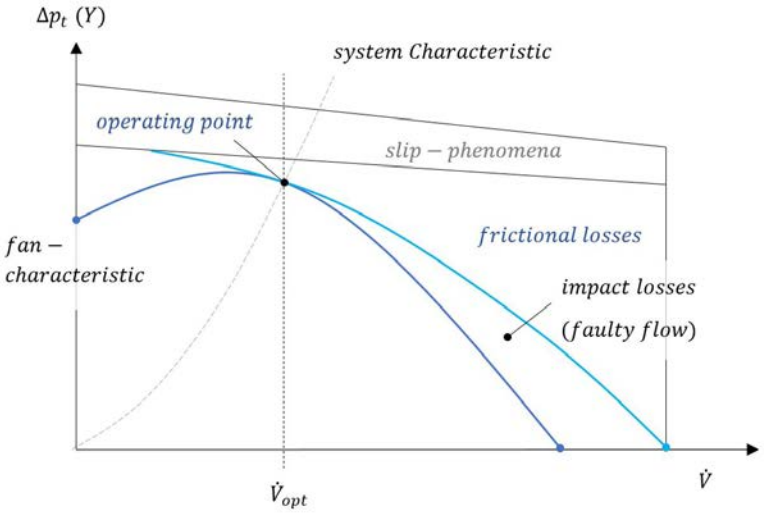

Figure 1. Volume flow total pressure characteristic diagram [7]

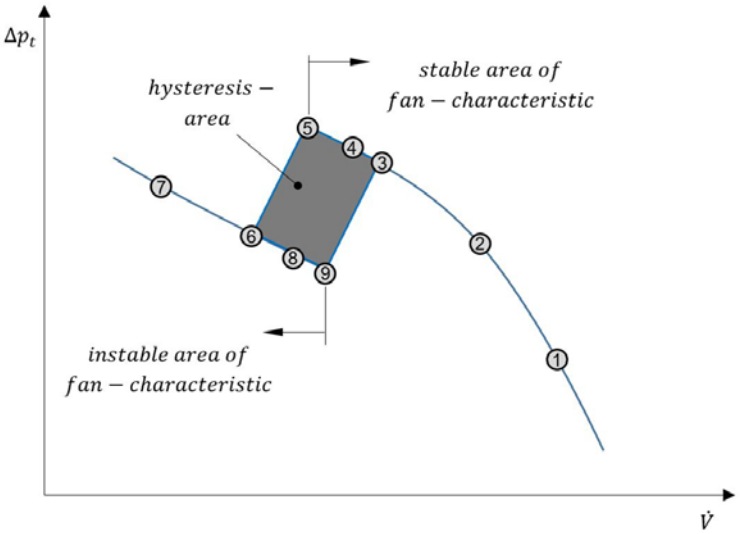

Figure 2. Characteristic of an axial fan [3]; Rotational speed: n = const.; Impeller blade angle: β_s = const.

D. Cause of flow separation

Figure 3 shows the profile section of an impeller blade with its velocity triangles at the operating points (1), (2) and (6) from **Figure 2**. It is recognisable that the velocity component c_1, which describes the volume flow though the fan decreases as result of a change in the system characteristic; this can be caused by throttling.

The size of the angle of attack α on the profile nose particularly influences the flow pattern on the aerofoils suction surface. If α has a favourable size according to the design of the profile, the air can overflow the profile with low impact. With increasing the angle of attack, it comes first to increase of lift force, but at the expense of worsening the glide ratio. If a maximum value of α is exceeded, the flow on the suction surface separates, which leads to a sudden drop in lift forces and a considerable deterioration in the gliding ratio [3].

Figure 5 shows a brief representation of the characteristics of a system with variable resistance and the characteristics of a fan with variable blade angles. By adjusting the angle of attack of the fan blades, different operating points can be achieved. If the fan design is correct, the operating points are in the range of high efficiency [3].

When changing the blade angle, the shape of the fan blade is disregarded. The shape of the optimum blade profile depends on the operating point of the fan with the required size volume flow, pressure difference and speed. Usually, this blade profile is not changeable and is picked out for the design point.

As a result, after an adjustment of the angle of attack, the velocity and direction of the flow is less favourable for fan blades with a good glide ratio. The buckle of the blade is then unfavourable because it is not operated at its design point. This produces air impact losses, thereby degrading efficiency and also giving rise to flow separation earlier. An adaptation of the blade profile is therefore crucial for a high efficiency.

Fans with adjustable blade angles are already well developed, but are rarely used because of the complexity and low advantages over speed control [12].

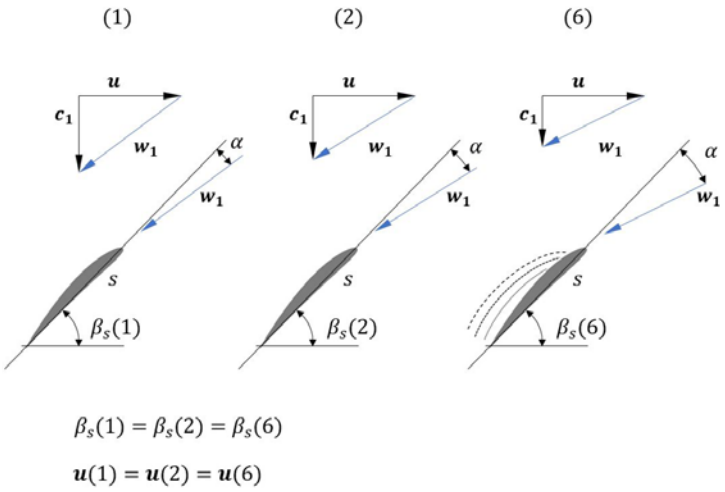

Figure 3. Flow triangles at the Impeller [3]

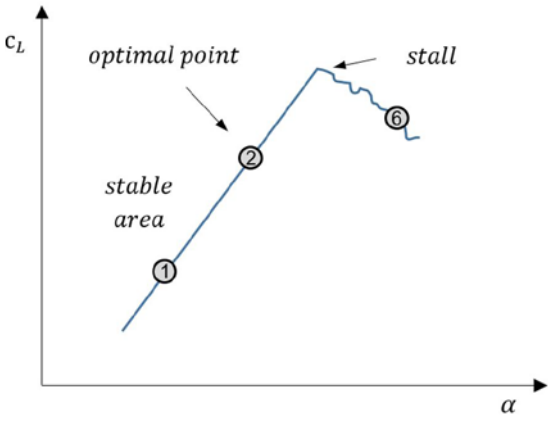

Figure 4. Lift polar schematically according to **Figure 2** [3]

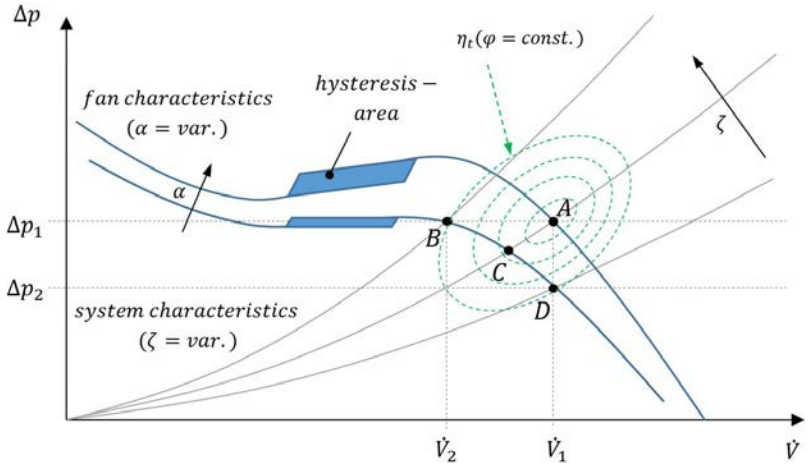

A→B: $\Delta p = \text{const}, \dot{V}_2 < \dot{V}_1$

A→C: $\zeta = \text{const}, \dot{V}_2 < \dot{V}_B < \dot{V}_1, \Delta p_2 < \Delta p_B < \Delta p_1$

A→D: $\dot{V} = \text{const}, \Delta p_2 < \Delta p_1$

Figure 5. Characteristic diagram with variable impeller blade angles [3].

If this blade angle adjustment succeeds in completing a camber adjustment function, the range of high efficiency can be significantly extended. The aim here is to control the adjustment of the profile curvature so that, depending on air speed, pressure and rotational speed, an increase of the range is achieved with high efficiency.

The aim is therefore the development of blades with adjustable blade angle, which have an additional function to change their profile curvature. In **Figure 6**, the improvement is shown schematically.

In order to produce different contours as faithfully as possible with an adaptive aerofoil, a specific subdivision of a profile (4-digit series NACA 4410 [1]) was applied by the superimposition of the parabolic arcs calculated for the construction. It turned out that in the division with three cuts, the shapes of different profiles can be simulated in a favourable approximation (**Figure 7**). The designed aerofoil consists of four parts, produced by a 3D printing process, which are connected to a common axis. To seal the resulting gaps on the surface of the aerofoil it has been covered with a nitryl-membrane.

All asymmetrically curved profile shapes have an optimal angle of attack with low impact losses. This corresponds to the $\boldsymbol{w_1}$ at a design-dependent profile curvature. With a mechanical drive, the curvature of the aerofoil adapts itself to its angle of attack, thereby eliminating the increase in the profile angle α with increased work requirements (**Figure 8**).

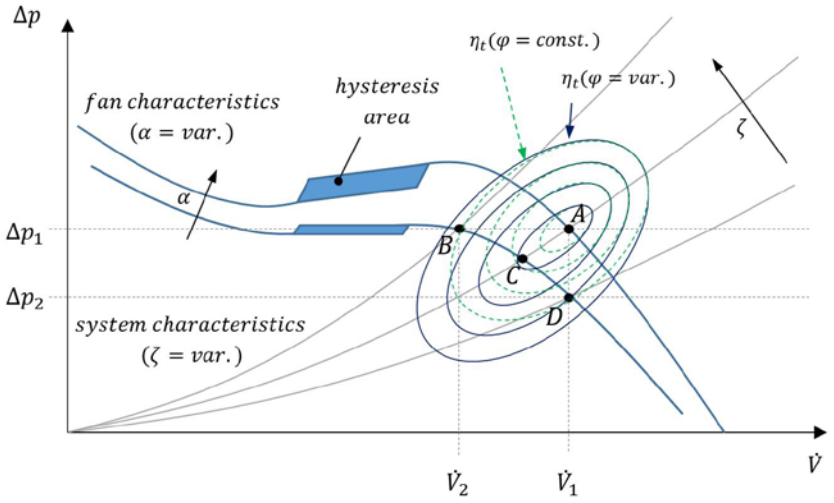

A→B: Δp = const, $\dot{V}_2 < \dot{V}_1$

A→C: ζ = const, $\dot{V}_2 < \dot{V}_B < \dot{V}_1$, $\Delta p_2 < \Delta p_B < \Delta p_1$

A→D: $\dot{V}$ = const, $\Delta p_2 < \Delta p_1$

Figure 6. Characteristic diagram schematically [3], extended with a variable blade camber $\varphi(\alpha)$ = var.

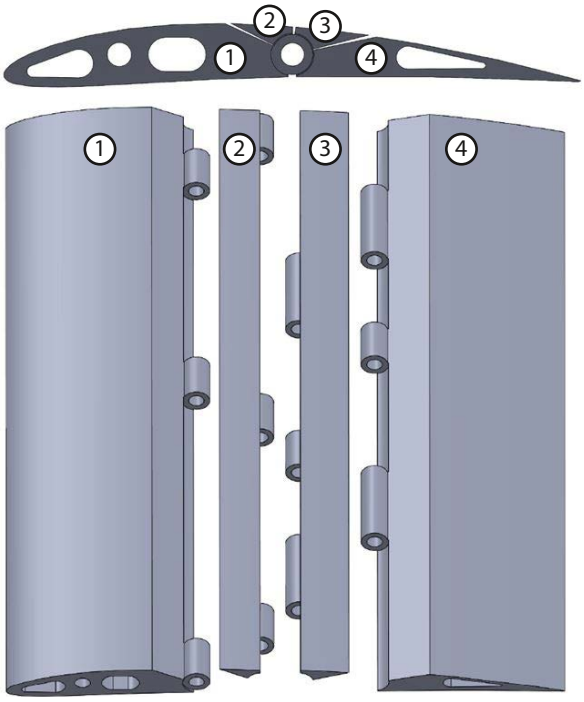

Figure 7. Idea for the construction of an adaptive aerofoil.

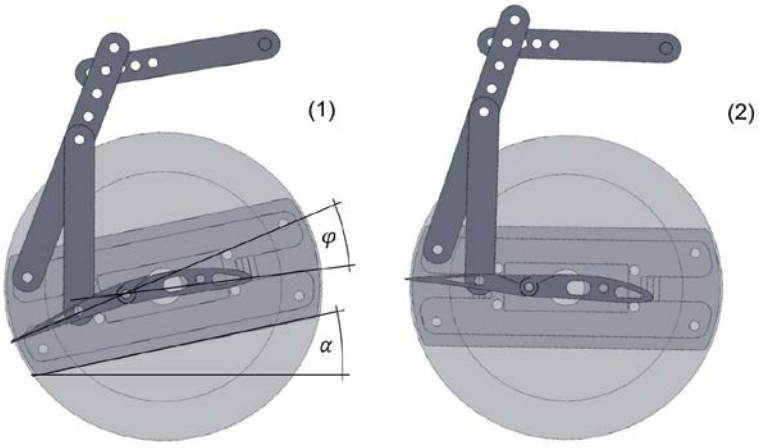

Figure 8. Working principle of adaptive camber drive ($\alpha_1 > \alpha_2$, $\varphi_1 > \varphi_2$).

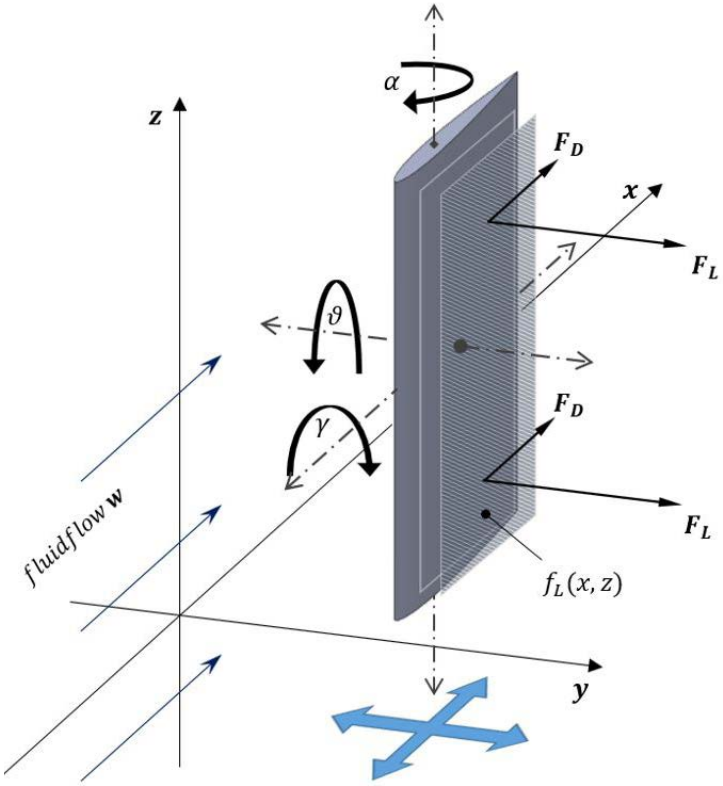

$$|F_L| = \iint f_L(x,z)dxdz$$

Figure 9. Representation of forces and degrees of freedom.

II. Experimental investigations

A. Measurement method

For the measurement of optimal lift-forces, which are determined by minimum values of the glide ratio ε, a test rig was developed. During the development of the test rig, six degrees of freedom of bodies in space were considered. These are the three coordinates of the body's centre of mass x, y, z, as well as the associated angles in space γ, ϑ, α [11]. **Figure 9** shows an aerofoil in dimetric exposition with the axial, rotational and pitching forces.

If aerofoils are examined by force measurement in wind tunnels, often one end of the aerofoil, similar to an airplane, is free in the flow. To account for these moments in the measurements, the aerofoil was attached at both ends, eliminating γ and ϑ. At the attachments of the aerofoil, a pair of forces then act accordingly to the priority of $|F_L|$ and $|F_D|$ (**Figure 10**). Side forces acting in the z-direction will be eliminated through the aerofoil's orientation when the leading edge of the aerofoil is orthogonal to w. Through the setting, the angle of attack α is fixed. The elimination of the degrees of freedom α, γ, ϑ and z, permits force exclusively on the measurement plane $x-y$, which are captured as lift and drag forces.

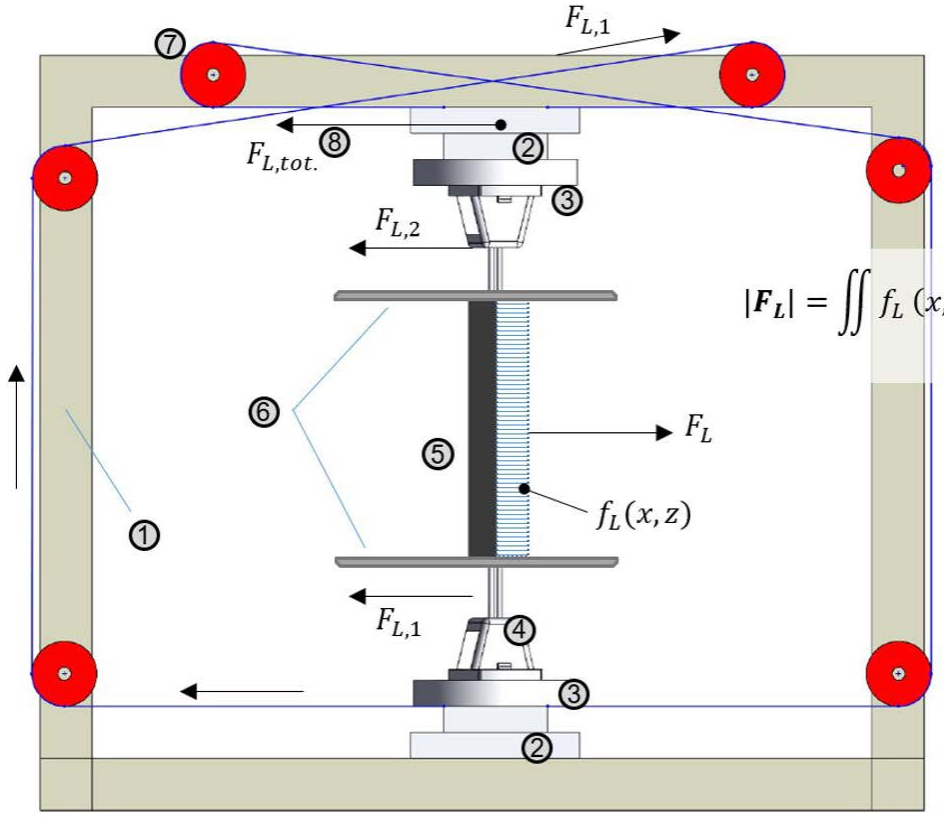

1 Stand
2 Gliding carriage
3 Rotary plate
4 Aerofoil attachment
5 Aerofoil
6 Side plates
7 Deflection roll
8 Position load cell

Figure 10. working principle test setup where $F_{L,tot} = |F_{L,1}| + |F_{L,2}|$.

B. Force measurements

Figure 11 shows the measured polars–F_L/α of the three aerofoils A (4410 rigid), B (2410 rigid) und C ([2-4]410 adaptive).

The light blue line in the graph describes the polar of the adaptive aerofoil C. Unlike the polars of the rigid aerofoils, which have a slight right curvature, the polar of the adaptive aerofoil having a relatively constant shape over the angle of attack passes.

Under the angles of attack of $1.5° \leq \alpha \leq 8°$ aerofoil C develops the same lift values as B. At values $1.5° \leq \alpha \leq 8°$, the polar runs between A and B and intersects A at $\alpha \approx 12°$. With a further increase in the angle of attack up to $\alpha \approx 20°$ the lift force increases to 10 N and remains at this value. Only at an angle of $\alpha \geq 25°$ is a very sudden drop in the lift observed.

The polars that can be seen in **Figure 12** show the lift values over the associated drag forces. Using a polar tangent through the origin, minimum values for the glide ratio ε can be indicated. Aerofoil A is therefore more efficient for larger lift forces, for smaller B is favourable.

The polar of aerofoil C is less curved than that of A and B, begins with the first reading at 1.2 N lift force, 0.4 N drag force and runs below the polar A and B. Before the decline of the lift value, a plateau at a force of 10 N can be recognised. It can be seen from the diagram that the drag values of the adaptive aerofoil C are higher than those of the rigid profiles.

C. PIV-measurements

For numbering the velocity of flow as well as for the detection of flow separation, the measurements at the adaptive aerofoil were extended with PIV analysis. The measurements also allow an additional assessment of the effects of the nitryl membrane on the surface flow.

Figure 13 shows the aerofoil under the angle of attack of $\alpha = 12.4°$ and the related camber of $\varphi = 20.9°$. The measurements

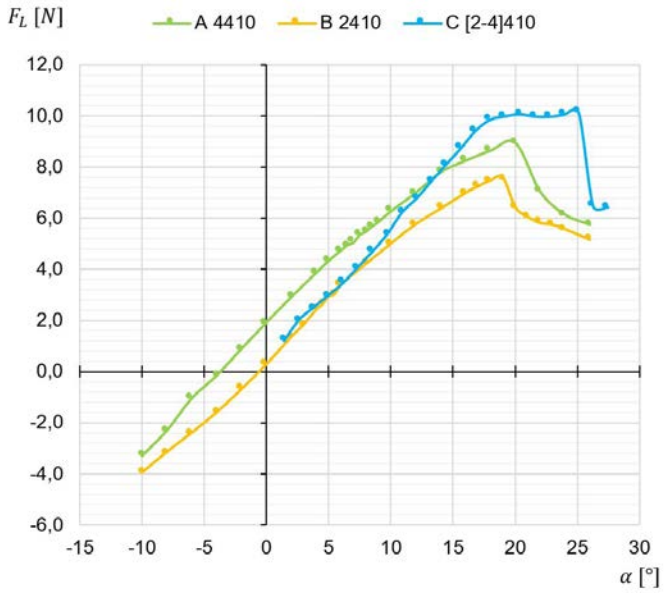

Figure 11. polars–F_L/α.

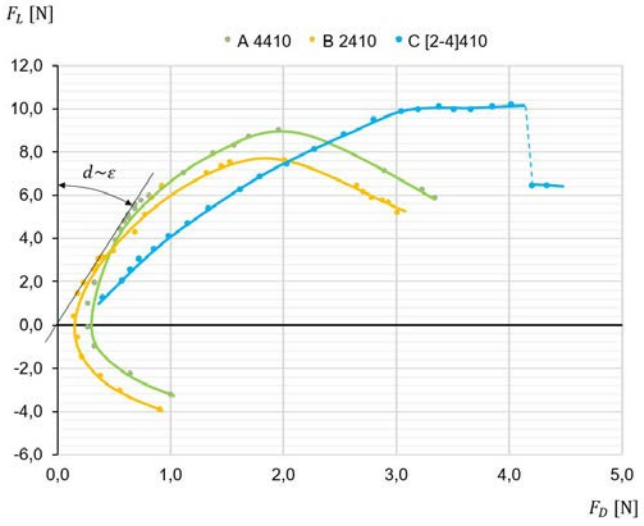

Figure 12. polars–F_L/F_D.

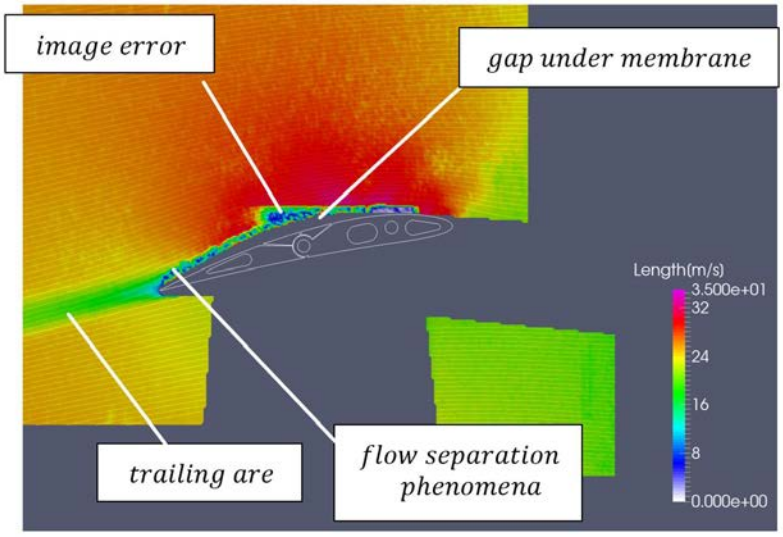

Figure 13. PIV flow mapping $\alpha = 12{,}4°$; $\varphi = 20{,}9°$.

showed that the stall-phenomena does not lead to flow separation despite an increased camber. The field of high velocities that increases at the leading edge and decreases glidingly with trailing edge indicates a favourable flow. Furthermore, a gap between aerofoil and air can be seen. The cause is that the surface rises due to the suction pressure, which increases the geometric thickness of the profile and can be seen as the reason for the increased drag forces according to **Figure 12**. Whether this has an influence on the lift distribution in addition to the increase in the form resistance, this must be investigated by future reference measurements.

Air velocities greater than 30 m / s can be detected near the suction surface at an incoming freestream velocity of 20 m/s.

III. Conclusion

The development of auto adaptive aerofoils for the use as a fan blade will improve the efficiency of flow machines.
It has been shown, that an aerofoil with a variable camber achieves an improved lift characteristic, especially at requirements outside the design point. This was proven by force measurements.
A high priority in the development of such adaptive aerofoils must be the preservation of a streamlined profile shape with all adjustable cambers. Investigations in the last century have produced many profile shapes, which have been extensively studied, described and optimised for the smallest values of ε. These forms are subject to a calculation method for defining a favourably curved skeleton line. In the adaptive aerofoil constructed in this work, the family of four-digit NACA profiles were chosen. The uniformly gentle curvature of the skeleton line, which is desired during the change in curvature, is shifted by a division into sections with a common point of rotation. The change in the curvature is transferred as a superposition to the skeleton line as **Figure 14** shows.

It can therefore be summarised that for the successful construction of an adaptive aerofoil, a low resistance through the flow-optimised contour and a high surface quality are decisive.

Which of the listed criteria outweighs and which effects the simulation of different cambers compared to the rigid original contours, on drag and lift forces, must show a number of further investigations. However, it is advisable to first investigate the effects of different surface materials on the drag forces on the aerofoil.

A. Outlook

The development of a seal for the surface of the adaptive aerofoil with less disruptive effects, for example with the help of a silicone joint or with a perforated membrane, should be strived for further research.
If it were possible to design the surface and shape of the adaptive aerofoil so that the drag force would be similar to that of A and B, the polar–F_L/F_D could look

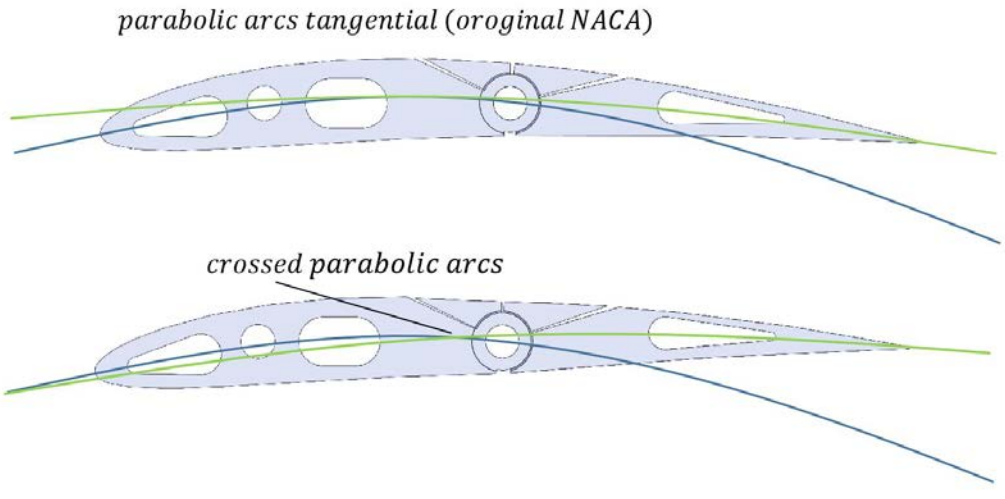

Figure 14. Superposition of the skeleton line.

like **Figure 15** and achieve optimum values for ε over large areas of F_L.

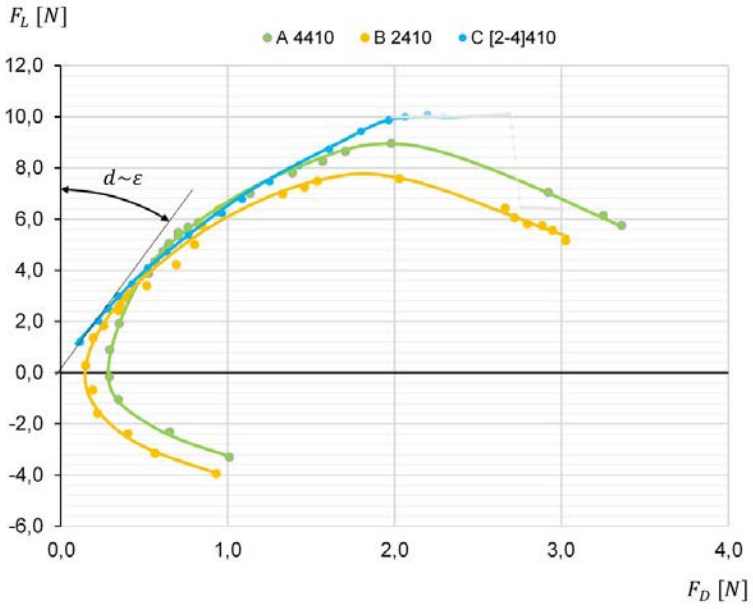

Figure 15. theoretic polar.

In the future, acoustic measuring tools for controlling the curvature of impeller blades would be conceivable in order to guide fans on the stable part of the fan characteristic curve. The development of innovative materials, such as shape memory alloy metals or advances in the applicability of elastomers could be an important part of fan design in the future. A replacement of complex mechanisms in the impeller would be conceivable [8].

Concluding remark

The research on adaptive aerofoils opens up great potential for the energy-saving use of axial fans. The upcoming challenge is the development of a suitable drive for the required camber control and its integration into the impeller blades.

This would be a large-scale success for a new generation of turbomachinery with dynamic characteristics. ■

References

[1] Airfoiltools.com: NACA 4-digit airfoil generator (NACA 4410 AIRFOIL) at http://airfoiltools.com/airfoil/naca4digit.

[2] Amtsblatt der Europäischen Union - DIE EUROPÄISCHE KOMMISSION: VERORDNUNG (EU) Nr. 327/2011(EU) Nr. 327/2011, 6.4.2011.

[3] Banzhaf, Hans-Ulrich (1986): „Stabile und instabile Betriebszustände bei Axialventilatoren" Heidenheim.

[4] Bischoff, Walter (2012): „Das kleine Bergbaulexikon" Essen.

[5] Carolus, Thomas (2013): „Ventilatoren Aerodynamischer Entwurf, Schallvorhersage, Konstruktion; mit … 42 Tabellen und zahlreichen Übungsaufgaben und Lösungen" Wiesbaden.

[6] ebmpapst (2017): „A3G630-AQ37-21 Betriebsanleitung Technische Daten" at http://img.ebmpapst.com/products/manuals/A3G630AQ3721-BA-GER.pdf?_ga=2.92730974.21386718.15059 86311-1265744298.1505986311.

[7] Epple, Philipp (2013): Prof. Dr.-Ing. Philipp Epple „Strömungsmechanische Grundlagen der Turbomaschinen" published.

[8] Kießlich, Robert (2017): „Entwurf und Untersuchung einer mittels Formgedächtnislegierungen-Aktoren veränderbaren Oberfläche, 24.04.2017" unpublished.

[9] Pfleiderer, Carl PETERMANN Hartwig (2005): Strömungsmaschinen, Berlin.

[10] Riegels, Friedrich Wilhelm (1958): Aerodynamische Profile Windkanal-Messergebnisse, Munich.

[11] TU-Dresden (2007): „Kraftmessungen an umströmten Körpern, in Script (Praktikum)Technische Universität Dresden Institut für Luft- und Raumfahrttechnik" unpublished.

[12] Witt&Sohn AG (2017): „im-lauf-verstellbare-schaufelntechnisches-know-how" at http://www.wittfan.de/de/ technisches-know-how/im-lauf-verstellbare-schaufeln.